Evolution of wave-function statistics from closed quantum billiards up to the open quantum dot limit: Application to the measurement of dynamical properties through imaging experiments

M. Mendoza and P. A. Schulz
Instituto de Física Gleb Wataghin, UNICAMP, Caixa Postale 6165, 13083-970 Campinas, São Paulo, Brazil
(Received 14 March 2006; published 6 July 2006)

We discuss the evolution of the electronic and scattering properties of a square billiard connected to the outside either by tunneling barriers or by progressively higher-conductance leads. The slightest connection already induces features of chaotic dynamics in the otherwise regular system. In the absence of large ensembles for energy level statistics or power spectrum analysis, we propose the distribution of the local densities to inspect the character of the underlying dynamics of a scattering state. We show that the wave-function statistics in wide open chaotic billiards strongly deviates from available predictions. The precursors of scarred wave functions are found in wave-function vortices that are tuned by the lead width.

DOI: 10.1103/PhysRevB.74.035304 PACS number(s): 73.23.−b, 05.45.Pq, 73.63.Kv

I. INTRODUCTION

The evolution of a quantum state connected to the environment, which is eventually a classical system, is one of the most basic questions in quantum mechanics. Tracing this evolution in mesoscopic systems has become a real possibility since the well-known conductivity measurements in semiconductor-based stadiums, revealing features of the underlying classical dynamics of the system.[1] In the past decade, semiconductor ballistic quantum dots with controlled connection to reservoirs have been used for investigations on the quantum to classical correspondence.[2]

Open quantum dots (OQDs) with a high number N of transmitting channels[3] are systems where the single-electron charging effects are not relevant and single-particle resonances should be robust with respect to electron-electron interactions.[4] These OQDs are candidates for wave-function mapping based either on resonance energy shifts[5] or on conductance shifts,[6] induced by atomic force microscope tips. This last procedure has been experimentally applied to imaging of quantum billiard states.[7] Therefore one could envisage the investigation of the statistical properties of wave functions in chaotic semiconductor-based mesoscopic billiards.[8] This possibility is highly desirable, since energy level statistics (successful in the Coulomb blockade regime[9]) are not applicable to OQDs and there is not a univocal relation between the fluctuations in the conductance and each billiard state. One the other hand, a conductance-fluctuation power spectrum analysis searching for periodic orbits[10] may also be misleading in grasping the dynamic features of OQDs, for the highly conducting leads could smear out important features in the Fourier transform of the conductance and therefore valuable information about periodic orbits could be lost. The development of wave-function imaging in quantum dots,[11] for the purpose of studying wave-function statistics,[12] could bring real OQDs to the status of reliable experimental testing tools for theories of quantum chaos. Such theories have been tested mainly in analogous systems, like microwave cavities.[13]

The probability distribution of probability densities (local density of states) of a given eigenstate, $P(\Psi^2)$, in closed chaotic cavities follows the Porter-Thomas (PT) distribution. In open cavities this behavior changes to the so-called generalized PT distribution (see Ref. 12). These statistical features have been investigated experimentally in closed and open microwave cavities, but with the restriction to few, $N < 10$, transmission channels. The aim of the present work is to numerically investigate the evolution of the wave-function statistics from closed quantum billiards up to the OQD limit, defined as dots connected to leads of large conductance, i.e., $G \gg 2e^2/h$, or $N \gg 1$, in the context of a possible measurement of dynamical properties through imaging experiments. We choose a square billiard, a well-studied system[14,15] that is completely regular when closed but presents chaotic features as soon as it is connected to the outside by tunneling barriers, showing a clear classical limit at $N \gg 1$. The present system is solely tuned by the opening width and not by changing an applied magnetic field[16] or the internal structure of the device.[17]

The numerical approach follows previous works: in order to get the conductance spectra of the OQD, transmission probabilities are calculated using recursive Green's function methods.[18,19] The local densities of states (LDOSs), in order to map $|\Psi^2|$, are also obtained within a Green's function approach.[20,5]

II. THE CONDUCTANCE SPECTRUM

Our system is defined on a square lattice of tight-binding s-like orbitals, as described elsewhere.[5] In the present energy scale, the lattice model emulates a system in the effective mass approximation (such as a semiconductor-based low-dimensional system). In all cases shown here, the OQD size is $L_x = L_y = 101a = 0.2\ \mu$m. The quantum point contacts (QPCs) are $L = 25a$ (500 Å) long and the width is varied from $w = 1a$ (20 Å) (tunneling limit) to $w = 51a$ (1000 Å) (wide open dots).

In Fig. 1 we present the conductance for a small energy range, varying the width w of the QPCs. For $w = 1a$, all the structures are tunneling resonances (lower panel). For $w = 5a$, we can see fluctuations on the second conductance plateau, while for wider leads, $w = 31a$ and $51a$, the resonances are on the $N = 13$ and 21 conductance plateaus, respectively.

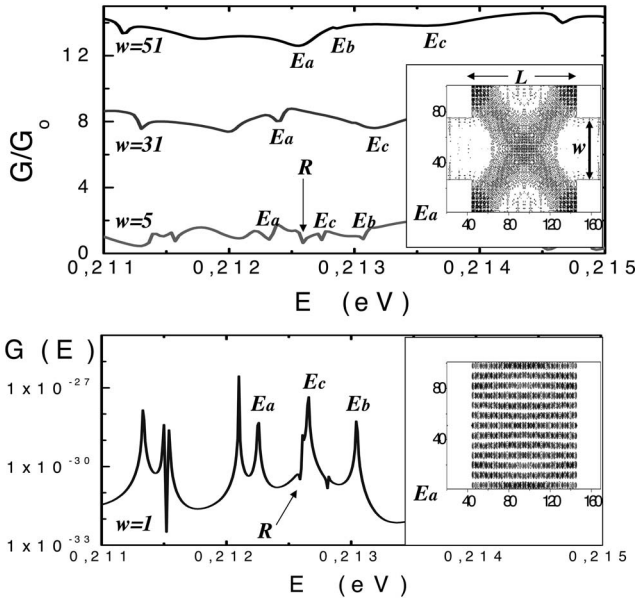

FIG. 1. Conductance for open square quantum dots for different lead widths w in a small energy range. Some of the resonances are labeled. The inset shows the open square quantum dot with the probability density (local density of states) at the energy of the E_a resonance for wide leads, $w=51a$ (upper panel), and very thin leads, $w=1a$ (lower panel).

By inspecting the probability density at the resonant energies, we are able to identify and follow each feature of the conductance as a function of QPC width. With increasing number of conductance channels, the resonances tend to become broader, associated with a diminution in the number of conductance fluctuations related to these resonances. Nevertheless, the line shape of several resonances can be followed, as a function of lead width w, and a nontrivial evolution can be seen. In particular, three examples are pointed out, E_a (associated with a scarred wave function, inset of Fig. 1), E_b [related to a bouncing ball orbit; see inset in Fig. 2(b)], and E_c [another case of localization of the eigenfunction around a classically allowed periodic orbit; see inset in Figs. 3(a)–3(d)]. It is interesting to notice that the E_a resonance corresponds to a completely regular single quantum state in the tunneling regime. For wide QPCs, this resonance evolves to an unstable periodic orbit associated with a clearly scarred wave function.

The energy range in Fig. 1 corresponds to a de Broglie wavelength approximately 20 times shorter than the lateral billiard dimension, $L \approx 20\lambda_{de\ Broglie}$, the figure of merit for the semiclassical limit. Also a resonance at ≈ 0.2 eV corresponds (for a closed square billiard with a side $L=101a$ $=0.2\ \mu$m and considering the electronic GaAs effective mass) to energies that would be the upper limit of ensembles of more than 700 eigenstates. It should be mentioned that the number of grid points used in the simulations is still adequate to correctly describe the nodes and antinodes of the eigenfunctions in this energy range. This is far inside the range in which the semiclassical limit would manifest itself. On the other hand, classical square billiards show strictly regular dynamics. Although rigorous analytical approaches

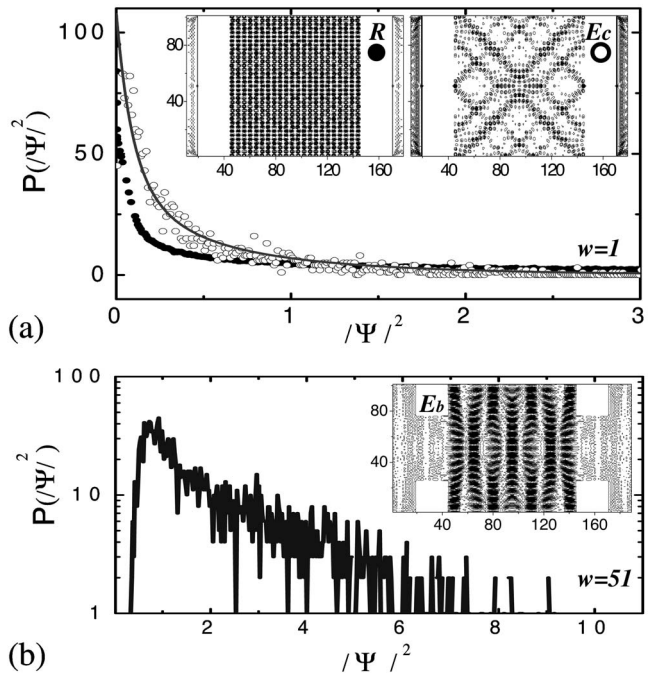

FIG. 2. (a) Probability distribution of probability densities associated with resonances of the slightly connected, $w=1a$, square billiard. Filled circles for the regular state R in Fig. 1 (corresponding probability density pattern in the left inset). Open circles for the E_c resonance in Fig. 1, following a PT distribution (continuous line), with the scarred pattern in the right inset. (b) Probability distribution of the probability density associated with a bouncing-ball-like resonance (E_b in Fig. 1) for wide leads, $w=51a$. Corresponding probability density pattern in the inset.

in the semiclassical limit are well understood,[14,15] associations between square billiard quantum solutions and classical periodic orbits have also been obtained by heuristic wave-

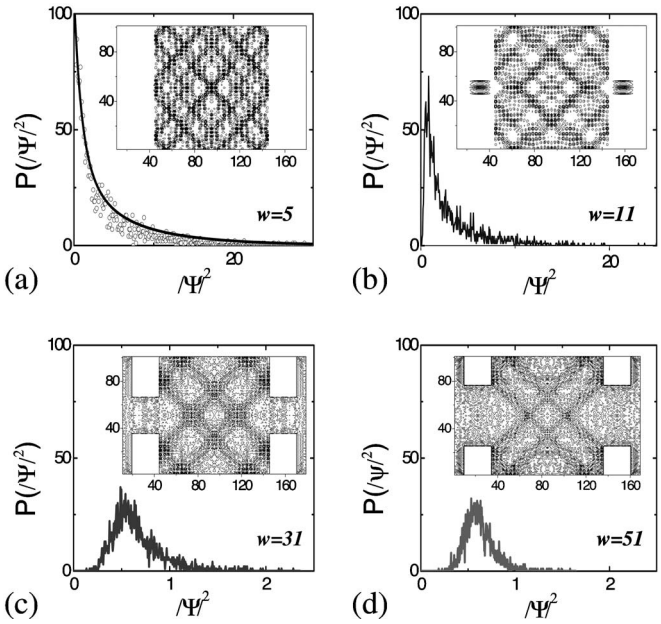

FIG. 3. As Fig. 2 for the resonance labeled E_c in Fig. 1 for wider connecting leads: $w=$(a) $5a$, (b) $11a$, (c) $31a$, and (d) $51a$.

function superposition,[21] while quantum chaotic features may be introduced in a closed square billiard by ripplelike shape perturbations.[22] By attaching the structures to leads the square billiard gets chaotic dynamics in this classical limit.[23] Since we are looking in a small energy interval, the number of resonances is not sufficient to proceed with a statistical analysis of energy spacings or from the power spectrum of the conductance, the usual tools in experimental investigations of chaotic behavior in the semiclassical and quantum limits. Therefore, we refer to the potential application of quantum state imaging as a tool for mapping the scattering state itself and label the corresponding dynamic behavior by means of a probability density distribution analysis, instead of current statistics,[24] which would be more involved from an experimental point of view.

III. BOTTLENECK OPENING OF SQUARE QUANTUM DOTS

Closed square billiards present a regular classical dynamics which is reflected in the quantum limit in a specific $P(\Psi^2)$ behavior: all eigenfunctions collapse on a single curve, illustrated by the filled circles in Fig. 2(a). With a proper shape perturbation, the square billiard starts to reveal a chaotic behavior,[22] which can be related to a PT distribution[12] for the wave-function intensity, the continuous line in Fig. 2(a). Here this shape perturbation is given by opening the square quantum dots, which also may induce chaos in the dynamics, as pointed out in previous work.[23] Three different opening regimes can be established: (i) Opening by tunneling, (ii) low conductance, and (iii) the commonly known OQDs connected by large conductance leads. From an experimental point of view, only the last regime—large conductance—can be well described by a single-electron model. However, the description of the two other regimes, within a single-particle framework, is important from the heuristic point of view, as well as for understanding the dynamics in related systems, like microwave cavities.

In the tunneling regime (thin leads, $w=1a$), the opening effects on the individual states are dramatically different, as can be seen in Fig. 2(a). The $P(\Psi^2)$ for the resonance indicated as R in Fig. 1 shows the closed system pattern [filled circles in Fig. 2(a)]. On the other hand, an almost overlapping resonance E_c shows already a strong mixing with a $P(\Psi^2)$ (open circles) following a generalized PT distribution (continuous line). This difference is clearly manifested in the corresponding probability density landscapes. The regular probability density pattern of the R resonance is depicted in the left inset of Fig. 2(a), while in the right inset we can see clear signatures of the formation of scars associated with the E_c structure in the conductance.

IV. WIDE OPEN SQUARE DOTS

Next we introduce low-conductance openings, namely, a few-channel lead connection $G \approx G_0 = 2e/h$. With this connection, strong fluctuations can be seen on the conductance plateau, related to the billiard eigenstates turning into resonances. We will focus now on the E_b resonance, associated

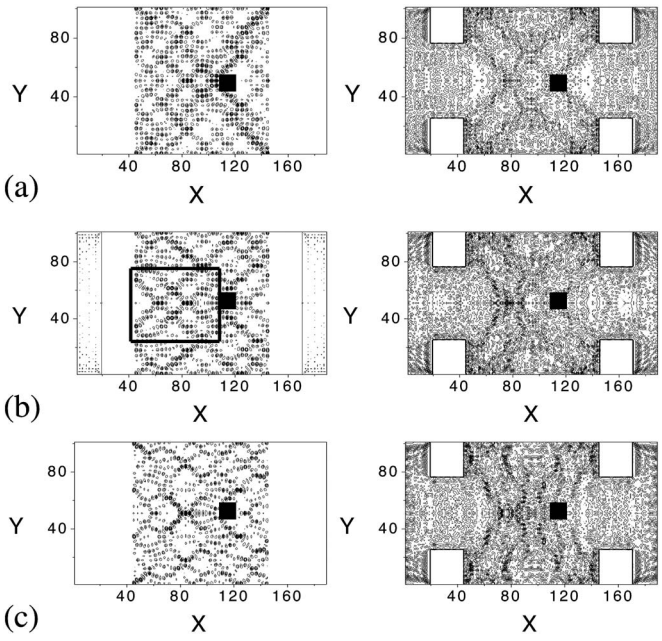

FIG. 4. Probability density plots at the E_c resonances in the presence of a potential bump at the indicated position (black squares). Left (right) column for narrow (wide) connecting leads, $w=1a$ ($51a$). Perturbation potential of $V=$(a) 0.05, (b) 0.1, and (c) 0.2 eV.

with bouncing ball orbits, which are not expected to follow a PT-like distribution for the probability density intensities.[25] However, an important general effect on $P(\Psi^2)$ can be observed: the progressive opening of the dot leads to a suppression of the probability for low probability densities with the eventual appearance of a threshold for sufficiently wide QPCs [Fig. 2(b)] (E_b for $w=51$). In other words, these states reveal an almost ergodically spread-out probability density. The case shown in Fig. 2(b) cannot be satisfactorily fitted by either the $P(\Psi^2)$ for regular systems, or the generalized PT one for chaotic systems.

One should also follow the evolution of the E_c resonance, with a pattern that evolves into a clear scar of periodic orbit for wide QPCs. The $P(\Psi^2)$ at the energy of the E_c resonance can be seen in Fig. 3. For $w=5a$ and $N=2$ there is negligible local density of states at the leads [Fig. 3(a)]. A chessboard scar pattern is present (see inset), as well as a vortex landscape,[22] also seen for other resonances not shown here, suggesting this vortex pattern as a precursor of unstable periodic orbit patterns. The $P(\Psi^2)$ depicted can still be described by a generalized PT distribution.

A dramatic change occurs in the limit of several open channels, i.e., a truly OQD with $G/G_0 \gg 1$, as in the conductance curve for $w=51a$ in Fig. 1. Now the E_c resonance becomes a very wide one at this energy scale and the corresponding probability density is ergodically spread out over the entire system. Nevertheless, a faint structure in the conductance is present and a scarred wave function around a periodic orbit characteristic of the geometry of the open square can be clearly seen. The surprise comes with the probability density distribution, completely different from a generalized PT distribution. In the inset of Fig. 3(d) we see

the probability density at the energy of the E_c resonance for $w=51a$. The corresponding $P(\Psi^2)$ shows a clear threshold at a finite intensity (characteristic for ergodicity), a smooth maximum at a finite value for the probability density, and an asymmetric tail. This asymmetric tail seems to be the remaining hint of a chaotic dynamics. The shape of the periodic orbit is stable against the opening of the contacts: the chessboard pattern continues to evolve until $w \approx 25$, after which the pattern remains essentially unchanged. Figures 3(b) and 3(c) show some intermediate situations, where the formation of a finite threshold for $P(\Psi^2)$ can be followed. Furthermore, in Fig. 3 it is interesting to observe the evolution of the vortexlike patterns. The probability density landscapes may suggest that the typical dimension of such vortexlike structures scales with the lead width w, eventually generating a scar pattern for wider contacts.

V. FINAL COMMENTS ON IMAGING

A completely different tuning of the system would be obtained by a potential spike at some position of the billiard, emulating the effect of an atomic force microscope tip for wave-function imaging purposes. The corresponding resonance at E_c in Fig. 1(a) (upper curve) presents an energy shift proportional to the probability density at the spike position (not shown here), which constitutes the imaging procedure described elsewhere.[5] Here we focus on the progressive breakdown of the periodic orbit with a potential spike (a $5a \times 5a$ square) at the indicated position (Fig. 4). The periodic orbit is robust for low-potential spikes and for the present case this orbit can still be clearly identified for a potential spike of $V=0.05$ eV [Fig. 4(a)]. A breakdown of the orbit, evolving to a scarred wave function with lower symmetry, occurs for higher-voltage spikes [Figs. 4(b) ($V=0.1$ eV) and 4(c) ($V=0.2$ eV)], specially for the wider-lead cases (right panel): now the potential spike acts like an effectively tunable barrier.[17] For thinner leads, the symmetry breaking is not so evident and evidences of self-similarity in the vortex pattern[7] are present.

A closed quantum system—a hard wall square billiard—starts to show chaotic features at the slightest opening to an external environment, which eventually lead to a clear classical limit, evidenced by robust periodic orbit scars in the local density of states. For high conductance and very short de Broglie wavelengths, the wave-function distribution statistics present completely different aspects that can only be reconciled to established analytical results at strict proper limits. Further work is necessary to properly describe the modification of the PT distribution for $N \gg 1$. In this scenario, the present results suggest an investigation tool for the underlying dynamics in mesoscopic systems based on the imaging of probability densities from conductance spectroscopy.

ACKNOWLEDGMENTS

This work has been supported by the Brazilian agency FAPESP. P.A.S. also acknowledges financial support from CNPq.

[1] C. M. Marcus, A. J. Rimberg, R. M. Westervelt, P. F. Hopkins, and A. C. Gossard, Phys. Rev. Lett. **69**, 506 (1992).
[2] D. K. Ferry, R. Akis, and J. P. Bird, Phys. Rev. Lett. **93**, 026803 (2004).
[3] W. A. Lin and R. V. Jensen, Phys. Rev. B **53**, 3638 (1996).
[4] T. Lundberg, J. E. F. Frost, K. F. Berggren, Z. L. Ji, C. T. Liang, I. M. Castleton, D. A. Ritchie, and M. Pepper, Semicond. Sci. Technol. **12**, 875 (1997).
[5] M. Mendoza and P. A. Schulz, Phys. Rev. B **71**, 245303 (2005).
[6] Y. Takagaki and K. H. Ploog, Phys. Rev. B **70**, 073304 (2004).
[7] R. Crook, C. G. Smith, A. C. Graham, I. Farrer, H. E. Beere, and D. A. Ritchie, Phys. Rev. Lett. **91**, 246803 (2003).
[8] P. W. Brouwer, Phys. Rev. E **68**, 046205 (2003).
[9] A. G. Huibers, S. R. Patel, C. M. Marcus, P. W. Brouwer, C. I. Duruoz, and J. S. Harris, Phys. Rev. Lett. **81**, 1917 (1998).
[10] R. G. Nazmitdinov, K. N. Pichugin, I. Rotter, and P. Seba, Phys. Rev. B **66**, 085322 (2002).
[11] S. Kicin, A. Pioda, T. Ihn, M. Sigrist, A. Fuhrer, K. Ensslin, M. Reinwald, and W. Wegscheider, New J. Phys. **7**, 185 (2005).
[12] H. Ishio, A. I. Saichev, A. F. Sadreev, and K.-F. Berggren, Phys. Rev. E **64**, 056208 (2001).
[13] Y.-H. Kim, U. Kuhl, H.-J. Stöckmann, and P. W. Brouwer, Phys. Rev. Lett. **94**, 036804 (2005).
[14] P. Pichaureau and R. A. Jalabert, Eur. Phys. J. B **9**, 299 (1999).
[15] L. Wirtz, C. Stamper, S. Rotter, and J. Burgdoerfer, Phys. Rev. E **67**, 016206 (2003).
[16] R. Akis, D. K. Ferry, and J. P. Bird, Phys. Rev. Lett. **79**, 123 (1997).
[17] C. S. Tang, W. W. Yu, and V. Gudmundsson, Phys. Rev. B **72**, 195331 (2005).
[18] H. U. Baranger, D. P. DiVincenzo, R. A. Jalabert, and A. D. Stone, Phys. Rev. B **44**, 10637 (1991).
[19] F. Sols, M. Macucci, U. Ravaioli, and K. Hess, J. Appl. Phys. **66**, 3892 (1989).
[20] S. Datta, Superlattices Microstruct. **28**, 253 (2000).
[21] Y. F. Chen, K. F. Huang, and Y. P. Lan, Phys. Rev. E **66**, 046215 (2002).
[22] W. Li, L. E. Reichl, and B. Wu, Phys. Rev. E **65**, 056220 (2002).
[23] J. A. Vergés, E. Cuevas, M. Ortuño, and E. Louis, Phys. Rev. B **58**, R10143 (1998).
[24] A. F. Sadreev, Phys. Rev. E **70**, 016208 (2004).
[25] A. F. Sadreev and K.-F. Berggren, Phys. Rev. E **70**, 026201 (2004).